The 2012 World Congress on
Advances in Civil, Environmental, and Materials Research (ACEM' 12)
Seoul, Korea, August 26-30, 2012

Prestressed Beam Condition Assessment Using Vibration Response Considering Bridge-Vehicle Interaction

*Zhi Sun[1)] and Zhongqiang Qi[2)]

[1)] *State Key Laboratory for Disaster Reduction in Civil Engineering, Shanghai, China*
[2)] *Department of Bridge Engineering, Tongji University, Shanghai, China*
[1)]*sunzhi1@tongji.edu.cn*

ABSTRACT

This paper presents a method to evaluate structure physical condition using bridge vibration response induced by vehicle. According to bridge design material, structural baseline finite element model is established firstly. The generally adopted 4DOF vehicle model is then integrated to setup a coupled dynamic system model considering bridge-vehicle interaction. Structural physical parameters, such as the structural flexural rigidity and the remaining prestress force, are then estimated by minimizing the least square error between bridge operational response measurement and the computed response from the baseline dynamic system model. The measurement noise on the accuracy of condition parameter estimation results will be discussed. The results from a numerical study verify that the proposed method is feasible and of good accuracy.

Keywords: prestressed beam, bridge vehicle interaction, operational response, parameter estimation

1. INTRODUCTION

Prestressed Concrete (PC) Beam Bridge is one of the most popular types of bridge in highway and railway system. Interest in its condition assessment keeps increased in recent years. Since the loss of its prestress force is one of the most observed condition degradation phenomenon, it is thus important to test this quantity continuously during its service life. Vibration test based method is proposed to be a good candidate for this

1) Research Fellow.
2) Postgraduate Student.

purpose. Saiidi et al. (1994) conducted a series of experimental study on PC beams and bridge to observe the variation trend of natural frequencies due to the variation of prestress force. The conclusion is that although the decrease of the prestress force should induce the increase of beam vibration frequencies according to the Euler beam vibration theory, the flexural rigidity softening effect due to prestress force decrease made the frequency variation show a decrease trend. Structural flexural rigidity variation due to prestress force change thus should be quantified before the identification of prestress force. Abraham et al. (1995) studied the effect of prestress force variation on the mode shape. The results observed showed that structural mode shape is not sensitive to the variation of structure prestress force. Lu and Law (2006) proposed a method for prestress force identification using structure vibration response based on sensitivity computation. Sun and Li (2008) made a further study on the identification of prestress force using response measurement considering the eccentricity of the prestress force. Besides vibration response based method, Kim et al. (2009) proposed to make use of structure impedance signature to identify the prestress force loss. Xu (2011) conducted a series of experimental study on PC beams to verify the feasibility of estimating structure prestress force using structural vibration response. The conclusion is structural flexural rigidity of the concrete beam is another variable which should be quantified during the process of prestress force identification.

In this paper, a method to identify the prestress force loss of PC beam bridge using vehicle induced bridge vibration response is proposed. Besides the prestress force, beam flexural rigidity is also updated during the identification process. A numerical study on a 30m-long simply supported beam bridge is conducted. The measurement noise on the accuracy of condition parameter estimation results will be discussed.

2. BRIDGE-VEHICLE COUPLED VIBRATION SYSTEM MODELING

Considering the bridge-vehicle coupled vibration system as shown in figure 1, the differential equation of motion of the system can be written as:

$$\begin{bmatrix} [M_b] & 0 \\ 0 & [M_v] \end{bmatrix} \begin{Bmatrix} \ddot{y}_b \\ \ddot{y}_v \end{Bmatrix} + \begin{bmatrix} [C_b] & 0 \\ 0 & [C_v] \end{bmatrix} \begin{Bmatrix} \dot{y}_b \\ \dot{y}_v \end{Bmatrix} + \begin{bmatrix} [K_b] & 0 \\ 0 & [K_v] \end{bmatrix} \begin{Bmatrix} y_b \\ y_v \end{Bmatrix} = \begin{Bmatrix} F_b \\ F_v \end{Bmatrix} \tag{1}$$

where $[M_b]$, $[C_b]$, and $[K_b]$ are the mass, damping and stiffness matrix of the bridge, respectively; $\{y_b\}$ and $\{F_b\}$ are the nodal response vector and equivalent nodal force vector of the bridge due to vehicle; $[M_v]$, $[C_v]$, and $[K_v]$ are the mass, damping and stiffness matrix of the vehicle cart, respectively; $\{y_v\}$ and $\{F_v\}$ are the response and force vectors of the vehicle.

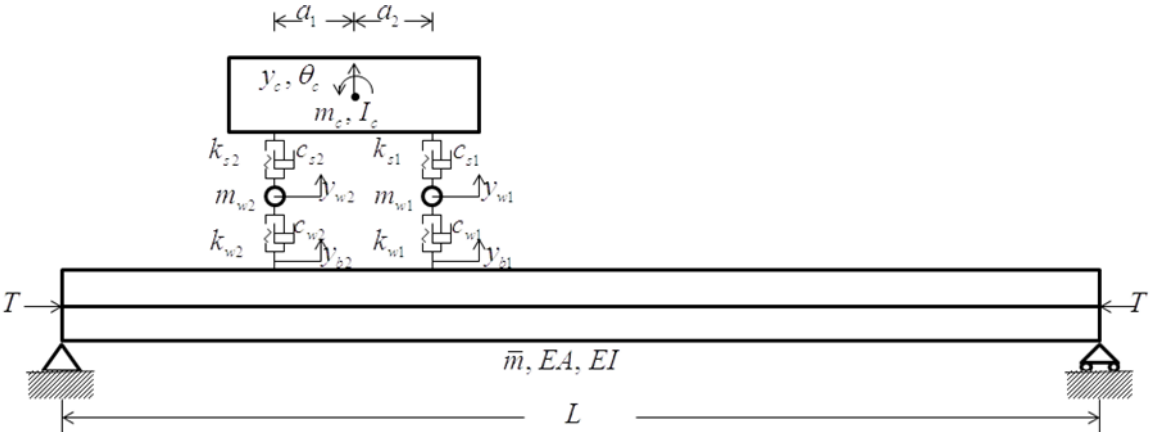

Figure 1: Bridge-vehicle coupled system

For the vehicle modeled as a 4DOF system, its mass, damping and stiffness matrices and force vector are of the following form

$$[M_v] = \begin{bmatrix} m_c & 0 & 0 & 0 \\ 0 & I_c & 0 & 0 \\ 0 & 0 & m_{w1} & 0 \\ 0 & 0 & 0 & m_{w2} \end{bmatrix}, \quad [C_v] = \begin{bmatrix} c_{s1}+c_{s2} & a_1c_{s1}-a_2c_{s2} & -c_{s1} & -c_{s2} \\ a_1c_{s1}-a_2c_{s2} & a_1^2c_{s1}+a_2^2c_{s2} & -a_1c_{s1} & a_2c_{s2} \\ -c_{s1} & -a_1c_{s1} & c_{s1}+c_{w1} & 0 \\ -c_{s2} & a_2c_{s2} & 0 & c_{s1}+c_{w2} \end{bmatrix} \tag{2}$$

$$[K_v] = \begin{bmatrix} k_{s1}+k_{s2} & a_1k_{s1}-a_2k_{s2} & -k_{s1} & -k_{s2} \\ a_1k_{s1}-a_2k_{s2} & a_1^2k_{s1}+L_2^2k_{s2} & -a_1k_{s1} & a_2k_{s2} \\ -k_{s1} & -a_1k_{s1} & k_{s1}+k_{w1} & 0 \\ -k_{s2} & a_2k_{s2} & 0 & k_{s1}+k_{w2} \end{bmatrix}$$
$$\{F_v\} = \{0 \quad 0 \quad c_{w1}\dot{y}_{b1}+k_{w1}y_{b1} \quad c_{w2}\dot{y}_{b2}+k_{w2}y_{b2}\}^T \tag{3}$$

where m_c and I_c are the mass and moment of inertia of the vehicle carriage, m_{w1} and m_{w2} are the masses of the front wheel and the suspension system and the back wheel and the suspension system of the vehicle, c_{s1} and c_{s2} are the damping coefficients of the suspension system of the front and the back wheels, c_{w1} and c_{w2} are the equivalent damping coefficients of the front and the back wheels, k_{s1} and k_{s2} are the stiffness coefficients of the suspension system of the front and the back wheels, k_{w1} and k_{w2} are the equivalent stiffness coefficients of the front and the back wheels, a_1 and a_2 are the lengths from the front and the back wheels to the gravity center of the carriage, y_c and θ_c are the vertical displacement and rotation of the vehicle carriage, y_{w1} and y_{w2} are the vertical displacements of the front and the back wheels, y_{b1} and y_{b2} are the vertical displacements of the bridge-front-wheel and bridge-back-wheel contacting points. If the contacting point is the element node of the bridge, the vertical displacement and the corresponding velocity are just the nodal vertical displacement and velocity of the bridge. If the contacting point is a point of the kth element of the bridge but not the elemental node point, the vertical displacement y_{bi} and the corresponding velocity $\dot{y}_{bi}$ can be obtained via the interpolation of bridge nodal responses using the Hermite shape

function as

$$y_{bi}\left(x,t\right)=\left[N(x)\right]\left\{\delta^{k}(t)\right\} \tag{4}$$

$$\dot{y}_{bi}(x,t)=\left[N(x)\right]\left\{\dot{\delta}^{k}(t)\right\}+\left[N'(x)\right]\left\{\delta^{k}(t)\right\}v \tag{5}$$

where $\left\{\delta^{k}(t)\right\}=\left\{y_{l}^{k}(t)\quad \theta_{l}^{k}(t)\quad y_{r}^{k}(t)\quad \theta_{r}^{k}(t)\right\}^{T}$ is the nodal response of the *k*th beam element, $\left\{\dot{\delta}^{k}(t)\right\}=\left\{\dot{y}_{l}^{k}(t)\quad \dot{\theta}_{l}^{k}(t)\quad \dot{y}_{r}^{k}(t)\quad \dot{\theta}_{r}^{k}(t)\right\}^{T}$ is the nodal velocity response of the *k*th beam element, $\left[N(x)\right]=\left[N_{1}(x)\ N_{2}(x)\ N_{3}(x)\ N_{4}(x)\right]^{T}$ is the Hermite shape function of the following form

$$\begin{aligned} N_{1}(x)&=1-3(\frac{x}{L})^{2}+2(\frac{x}{L})^{3} \qquad & N_{2}\left(x\right)&=x(1-\frac{x}{L})\\ N_{3}(x)&=3(\frac{x}{L})^{2}-2(\frac{x}{L})^{3} \qquad & N_{4}\left(x\right)&=\frac{x^{2}}{L}(\frac{x}{L}-1)\end{aligned} \tag{6}$$

$\left[N'(x)\right]=\left[N_{1}'(x)\ N_{2}'(x)\ N_{3}'(x)\ N_{4}'(x)\right]^{T}$ is the first differentiation of the Hermite shape function, and *v* is the driving speed of the vehicle.

For the eccentrically prestressed beam bridge, it can be modeled using the beam elements of the following stiffness and mass matrices:

$$\left[K_{b}\right]=\left[\bar{K}\right]+\left[K_{G}\right]=\sum_{j=1}^{n}\left(\left[\bar{k}^{j}\right]+\left[k_{G}^{j}\right]\right),\quad \left[M_{b}\right]=\sum_{j=1}^{n}\left[m^{j}\right] \tag{7}$$

where $\left[\bar{K}\right]$ and $\left[K_{G}\right]$are the global elastic stiffness matrix and geometric stiffness matrix caused by axial force; $\left[\bar{k}^{j}\right]$, $\left[k_{G}^{j}\right]$ and $\left[m^{j}\right]$ are the elemental elastic stiffness matrix, elemental geometric stiffness matrix due to axial prestress force, and elemental mass matrix as shown below.

$$\left[\bar{k}^{j}\right]=\frac{2EI}{L^{3}}\begin{pmatrix}6 & 3L & -6 & 3L\\ 3L & 2L^{2} & -3L & L^{2}\\ -6 & -3L & 6 & -3L\\ 3L & L^{2} & -3L & 2L^{2}\end{pmatrix},\ \left[k_{G}^{j}\right]=\frac{T}{30L}\begin{pmatrix}36 & 3L & -36 & 3L\\ 3L & 4L^{2} & -3L & -L^{2}\\ -36 & -3L & 36 & -3L\\ 3L & -L^{2} & -3L & 4L^{2}\end{pmatrix},$$

$$\left[m^j\right]=\frac{\bar{m}L}{420}\begin{pmatrix}156 & 22L & 54 & -13L\\ 22L & 4L^2 & 13L & -3L^2\\ 54 & 13L & 156 & -22L\\ -13L & -3L^2 & -22L & 4L^2\end{pmatrix} \tag{8}$$

where L, $\bar{m}$ and T are the length, the mass per unit length and the prestressed force of the element, respectively; EI and EA are the flexural rigidity and compressive rigidity of the cross section of the beam; d_2 and d_1 are the deflections at the left end and the right end of the element, respectively. Since the prestress force T is set to be positive, the item $\left[K_G\right]$ is minus in Eq. (2) to indicate the softening effect of prestress force on stiffness. The damping matrix $\left[C_b\right]$ is assumed to be Rayleigh damping expressed as the following

$$\left[C_b\right]=\alpha_0\left[M_b\right]+\alpha_1\left[K_b\right] \tag{9}$$

where α_0 and α_1 can be expressed as

$$\alpha_0=\frac{2\omega_1\omega_2(\xi_1\omega_2-\xi_2\omega_1)}{\omega_2^2-\omega_1^2}, \quad \alpha_1=\frac{2(\xi_2\omega_2-\xi_1\omega_1)}{\omega_2^2-\omega_1^2} \tag{10}$$

where ω_1 and ω_2 are structural natural frequencies of the first and second vertical bending vibration modes; ξ_1 and ξ_2 are the corresponding modal damping ratios. Bridge nodal force vector $\left\{F_b\right\}$ is a vector with the non-zero terms of $\left\{F_b^k\right\}$ if the wheel force of the vehicle P_{bi} is acted on the kth beam element of the bridge

$$\left\{F_b^k\right\}=\left[N(x)\right]P_{bi} \tag{11}$$

$$P_{b1}=m_{w1}g+\frac{a_2}{a_1+a_2}m_cg+\frac{a_2}{a_1+a_2}m_c\ddot{y}_c+\frac{I_c}{a_1+a_2}\ddot{\theta}_c+m_{w1}\ddot{y}_{w1} \tag{12}$$

$$P_{b2}=m_{w2}g+\frac{a_1}{a_1+a_2}m_cg+\frac{a_1}{a_1+a_2}m_c\ddot{y}_c-\frac{I_c}{a_1+a_2}\ddot{\theta}_c+m_{w2}\ddot{y}_{w2} \tag{13}$$

where P_{b1} and P_{b2} are the forces applied by the front and back wheel on the bridge, respectively.

Obtaining the governing equation for the coupled vibration system, the Newmark-β method is then employed to solve the equation and compute structure dynamic responses.

3. PRESTRESSED BEAM BRIDGE CONDITION ASSESSMENT

Considering the condition degradation of a concrete bridge during its service life, the most generally occurred phenomena are the flexural rigidity reduction due to concrete cracking and the prestress force loss due to steel wire relaxation. In this study, the related physical quantities, *EI* and *T,* are thus selected for the inverse identification purpose.

Take the first order differentiation on the two sides of the equation of motion of the bridge with respect to *EI* and *T* respectively; the following two equations are obtained

$$[M_b]\left\{\frac{\partial \ddot{y}_b}{\partial T}\right\}+[C_b]\left\{\frac{\partial \dot{y}_b}{\partial T}\right\}+[K_b]\left\{\frac{\partial y_b}{\partial T}\right\}+\left[\frac{\partial C_b}{\partial T}\right]\{\dot{y}_b\}+\left[\frac{\partial K_b}{\partial T}\right]\{y_b\}=0 \tag{14}$$

$$[M_b]\left\{\frac{\partial \ddot{y}_b}{\partial (EI)}\right\}+[C_b]\left\{\frac{\partial \dot{y}_b}{\partial (EI)}\right\}+[K_b]\left\{\frac{\partial y_b}{\partial (EI)}\right\}+\left[\frac{\partial C_b}{\partial (EI)}\right]\{\dot{y}_b\}+\left[\frac{\partial K_b}{\partial (EI)}\right]\{y_b\}=0 \tag{15}$$

It is noted that $[M_b]$ is not dependent on *T*, and thus the partial derivative $\frac{\partial M_b}{\partial T}$ in Eq. (14) disappears. According to Eq. (8) and Eq. (9),

$$\begin{aligned}
&\frac{\partial[K_b]}{\partial T}=\frac{\partial\left(\left[\bar{K}\right]+[K_G]\right)}{\partial T}=\frac{\partial[K_G]}{\partial T} \qquad \frac{\partial[K_b]}{\partial (EI)}=\frac{\partial\left(\left[\bar{K}\right]+[K_G]\right)}{\partial (EI)}=\frac{\partial\left[\bar{K}\right]}{\partial (EI)}\\
&\frac{\partial[C_b]}{\partial T}=\frac{\partial\left(\alpha_0[M_b]+\alpha_1[K_b]\right)}{\partial T}=\alpha_1\frac{\partial[K_b]}{\partial T} \qquad \frac{\partial[C_b]}{\partial (EI)}=\frac{\partial\left(\alpha_0[M_b]+\alpha_1[K_b]\right)}{\partial (EI)}=\alpha_1\frac{\partial[K_b]}{\partial (EI)}
\end{aligned} \tag{16}$$

To identify structural physical variables, structural response measured from different DOFs are required to be measured. Equations (14) and (15) can thus be transformed to be

$$[M_b]\left\{\frac{\partial \ddot{y}_b}{\partial T}\right\}+[C_b]\left\{\frac{\partial \dot{y}_b}{\partial T}\right\}+[K_b]\left\{\frac{\partial y_b}{\partial T}\right\}=-\frac{\partial[K_G]}{\partial T}(\alpha_1\{\dot{y}_b\}+\{y_b\}) \tag{17}$$

$$[M_b]\left\{\frac{\partial \ddot{y}_b}{\partial (EI)}\right\}+[C_b]\left\{\frac{\partial \dot{y}_b}{\partial (EI)}\right\}+[K_b]\left\{\frac{\partial y_b}{\partial (EI)}\right\}=-\frac{\partial\left[\bar{K}\right]}{\partial (EI)}(\alpha_1\{\dot{y}_b\}+\{y_b\}) \tag{18}$$

Solve the above two equations under the pseudo-excitation on the left hand of the equation, the sensitivity responses can be computed. According to the definition of sensitivity, the relationship between the dynamic response difference $\{\delta y_{bg} \quad \delta y_{bf}\}^T$ and the physical variable increment $\{\delta T \quad \delta(EI)\}^T$ is

$$\begin{bmatrix} \dfrac{\partial y_{bg}}{\partial T} & \dfrac{\partial y_{bg}}{\partial (EI)} \\ \dfrac{\partial y_{bf}}{\partial T} & \dfrac{\partial y_{bf}}{\partial (EI)} \end{bmatrix} \begin{Bmatrix} \delta T \\ \delta (EI) \end{Bmatrix} = \begin{Bmatrix} \delta y_{bg} \\ \delta y_{bf} \end{Bmatrix} \tag{19}$$

Then physical variable increment $\{\delta T \quad \delta(EI)\}^T$ can then be solved from Eq. (19) using the minimum least square method.

Since the relationship between physical variable and structure response is nonlinear, numerical iterations are required to get converged results. The convergence principle to stop the iteration is set to be

$$\frac{|\delta T_k|}{|T_k|} \le r \quad \& \quad \frac{|\delta (EI)_k|}{|(EI)_k|} \le r \tag{20}$$

where the threshold value *r* is set to be 1×10^{-5}.

4. CASE STUDY ON PTESTRESS FORCE IDENTIFICATION

To verify the proposed method, a numerical study on a simply-supported beam is conducted. The length of the beam is 30 m. The mass per meter and flexural rigidity of the beam are 1500 kg/m and 2 *GN*m*^{2}, respectively. The initial prestress force applied on the bridge is set to be 5 *MN*. The natural frequencies of the first two vertical vibration modes are 14.032, and 52.079 *Hz*, which are obtained by taking eigenvalue analysis on the FEM model of the bridge. The damping ratios of these two modes are set to be 2% to compute the Rayleigh damping coefficients. For the 4DOF vehicle, its physical parameters are set to be $m_c = 32025kg$, $I_c = 82615.67kg\cdot m^2$, $m_{w1} = 480kg$, $m_{w2} = 950kg$, $a_1 = 0.95m$, $a_2 = 2.65m$, $k_{s1} = 1.7\times10^5 N/m$, $k_{s2} = 4.8\times10^5 N/m$, $k_{w1} = 9.5\times10^5 N/m$, $k_{w2} = 1.9\times10^6 N/m$, $c_{s1} = 1.7\times10^5 kg/s$, $c_{s2} = 1.4\times10^4 kg/s$, $c_{w1} = c_{w2} = 0kg/s$. Dynamic response analysis for the coupled system is then computed. Figure 2 shows the computed vertical displacement response at the mid-point of the bridge when the 4DOF vehicle passes through the bridge in the velocities of 5 m/s, 10 m/s, 15 m/s, and 20 m/s. During the computation, the time increment is set to be 0.01s.

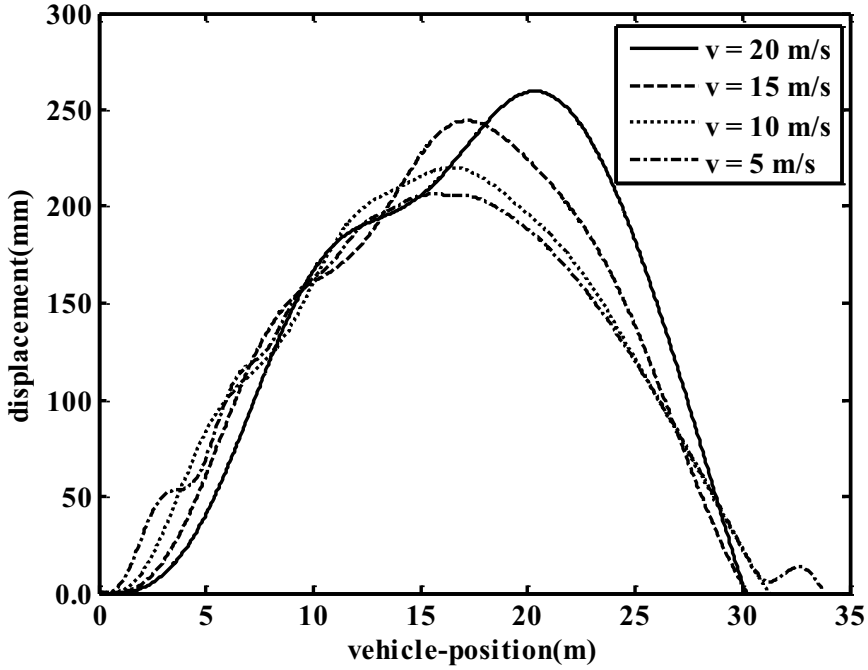

Figure 2**:** The computed vertical displacement response of the mid-point of the bridge when the vehicle pass through the bridge in different velocities

For physical variable identification, figure 3 illustrates the procedure when *T* and *EI* are reduced to 4.625 *MN* and 1.326 $GN*m^2$, respectively. Structural responses under vehicle excitation are then simulated to be measured. In the case study, structural vertical displacement responses at the 2/5 point and mid-point of the bridge excited by the vehicle in a speed of 5 m/s to pass through the bridge are measured. Since the measured response is different to the baseline response as shown in Fig. 3a, the sensitivity responses to *T* and *EI* at these two DOFs are computed (as shown in Fig. 3b and Fig. 3c). The iterative inverse mapping process is then conducted to update *T* and *EI* of the baseline model until the numerical responses are converged to the simulated measurement responses (as shown in Fig. 3d).

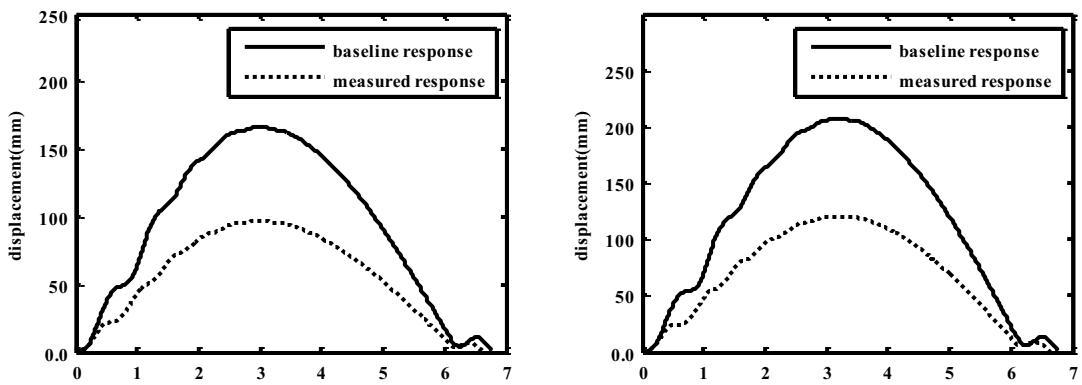

(a1) (a2)

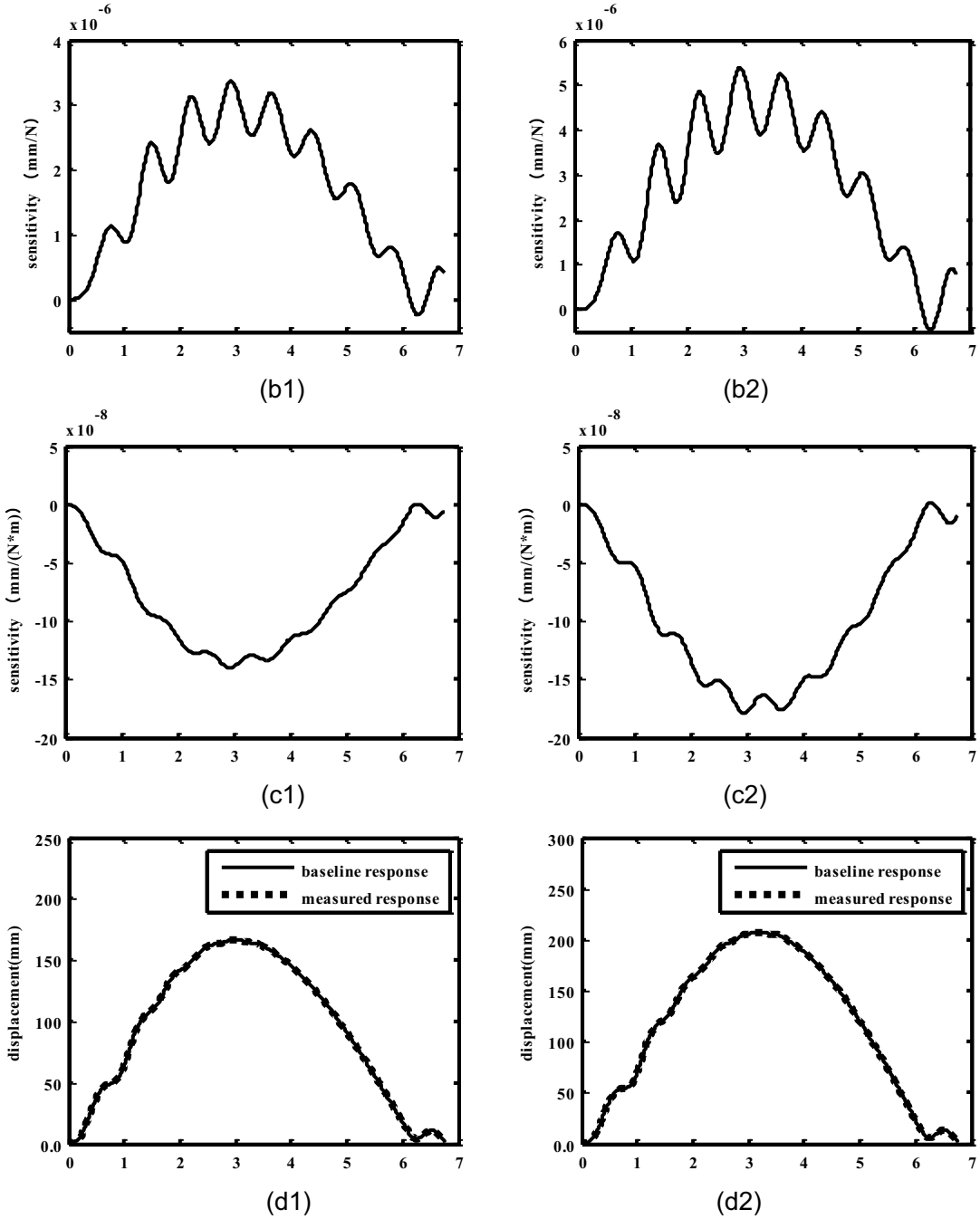

Figure 3: The identification procedure: comparison of the baseline response and the measured response at the 2/5 point (a1) and at the mid-point (a2) of the bridge; sensitivity response to *T* at the 2/5-point (b1) and at the mid-point (b2) of the bridge; sensitivity response to *EI* at the 2/5-point (c1) and at the mid-point (c2) of the bridge; comparison of the converged response and the measured response at the 2/5 point (d1) and at the mid-point (d2) of the bridge.

To verify the accuracy of the proposed method, ten bridge condition degradation

cases are randomly generated among the region of [0 40%] of *T* and *EI* reduction. Table 1 lists the identification results for those cases. As shown in the table, the identification results are exactly the same as the pre-generated target value if the first 4 effective numbers of the target value and the identified value are compared.

Table 1: The identification results for different condition degradation cases

Case Number	Target Value		Identified Value		Number of Iterations
	T (MN)	*EI (GN*m²)*	$\bar{T}$ *(MN)*	$\overline{EI}$ *(GN*m²)*	
1	4.625	1.326	4.625	1.326	9
2	4.805	1.974	4.805	1.974	6
3	3.255	1.964	3.255	1.964	7
4	4.820	1.588	4.820	1.588	7
5	4.260	1.838	4.260	1.838	7
6	3.195	1.340	3.195	1.340	9
7	3.555	1.536	3.555	1.536	8
8	4.090	1.930	4.090	1.930	6
9	4.910	1.832	4.910	1.832	7
10	4.925	1.966	4.925	1.966	6

To further verify the accuracy of the proposed method in noisy condition, 4 levels of noise (from 1%, 5%, 10% to 20% of structural vibration responses), are added to the response measurements. The algorithm is then employed to identify the physical variables using the noise-polluted response measurements. For each level of noise, 50 white noise records are randomly generated and 50 physical variable identification processes are conducted. A statistical analysis was then conducted to compute the mean and the standard deviation of the identified physical variables. Table 2 lists the results. As shown in the table, if the noise intensity is smaller than 5%, the identified values are accurate enough as the mean values match with the pre-set target value quite well and the standard deviations are quite small. If the noise intensity is increased, more identification error is observed. However, even when the noise intensity goes to 20%, the relative errors for *T* and *EI* are still 2.16% and 0.67%, which is an acceptable level. Therefore, the proposed method is noise insensitive.

Table 2: The identification results when the signals are polluted by different levels of noise

Noise intensity	Target value		Identified value			
	T (*MN*)	*EI* (*GN*m²*)	$\bar{T}$ (*MN*)	$\overline{EI}$ (*GN*m²*)	σ_T (*MN*)	σ_{EI} (*GN*m²*)
1 %	4.625	1.326	4.623	1.326	0.022	0.002
5 %	4.625	1.326	4.628	1.325	0.078	0.007
10 %	4.625	1.326	4.683	1.321	0.231	0.021
20 %	4.625	1.326	4.725	1.317	0.469	0.043

CONCLUSION

This paper presents a method to assess bridge physical condition degradation by monitoring vehicle induced structural vibration response. According to the design material, bridge baseline model is established firstly. Structural physical parameters, such as structural flexural rigidity and remaining prestress force, are then estimated by minimizing the least square error between bridge operational response measurement and the numerical response from the baseline model. A numerical study on a 30m-long simply supported beam bridge is conducted. The results verify the accuracy and efficiency of the proposed method. If the response measurements are polluted by different levels of noise, the identification results shown that the proposed method is immunity from 5% noise.

ACKNOWLEDGEMENT

This research was supported by the Rising-star Tracking Program of Shanghai Commission of Science and Technology (Grant No. 09QH1402300).

REFERENCE

Abraham, M. A.; Park, S. Y.; Stubbs, N. (1995), “Loss of prestress prediction on nondestructive damage location algorithms”, *SPIE, Smart Structures and Materials*, vol. **2446**, pp. 60–67.

Kim, J. T.; Park, J. H.; Hong, D. S.; Cho, H. M. and Na, W. B. (2009), “Vibration and impedance monitoring for prestress-loss prediction in PSC girder bridges”, *Smart Structures and Systems*, vol. **5**, No. 1, pp. 81–94.

Lu, Z. R.; Law, S. S. (2006), “Identification of prestress force from measured structural responses”, *Mechanical Systems and Signal Processing*, vol. **20**, issue. 8, pp. 2186–2199.

Saiidi, M.; Douglas, B.; Feng, S. (1994), “Prestress force effect on vibration frequency of concrete bridges”, *Journal of Structural Engineering-ASCE*, vol. **120**, no. 7, pp. 2233–2241.

Sun, Z.; Li, Z. (2008), “Load carrying capacity assessment of prestressed concrete beam bridge from structural forced vibration response”, *Proceeding of IABSE,* vol. **95**, pp. 502–503.

Xu, J. L. (2011), *Experimental Study of Prestress Force Identification of PC Beam Based on Vibration Test*, Master Thesis of Tongji University, Shanghai, China.